Journal of Power Sources 196 (2011) 3655–3658

Contents lists available at ScienceDirect

Journal of Power Sources

journal homepage: www.elsevier.com/locate/jpowsour

Short communication

Highly dispersed sulfur in ordered mesoporous carbon sphere as a composite cathode for rechargeable polymer Li/S battery

Xiao Liang, Zhaoyin Wen*, Yu Liu, Hao Zhang, Lezhi Huang, Jun Jin

CAS Key Laboratory of Energy Transforming Materials, Shanghai Institute of Ceramics, Chinese Academy of Sciences, No. 1295 Dingxi Road, Shanghai 200050, PR China

ARTICLE INFO

Article history:
Received 20 July 2010
Received in revised form
22 November 2010
Accepted 16 December 2010
Available online 23 December 2010

Keywords:
Sulfur composite cathode
Mesoporous carbon sphere
Lithium sulfur battery

ABSTRACT

A mesoporous carbon sphere with the uniform channels (OMC) is employed as the conductive matrix in the sulfur cathode for the lithium sulfur battery based on all-solid-state $PEO_{18}Li(CF_3SO_2)_2N$–10 wt%SiO_2 electrolyte. Cyclic voltammograms (CV) and electrochemical impedance spectrum (EIS) suggest that the electrochemical stability of the S-OMCs is obviously superior to the pristine sulfur cathode. The S-OMCs composite shows excellent cycling performance with a reversible discharge capacity of about 800 mAh g^{-1} after 25 cycles. This would be attributed to an appropriate conductive structure in which the active sulfur is highly dispersed in and contacted with the OMCs matrix.

1. Introduction

From portable batteries for small-size electronic devices and power sources for electrical vehicles, there has been strong incentive to develop a high specific energy lithium battery. Lithium sulfur battery is the most promising candidate for its high theoretical specific capacity of 1675 mAh g^{-1}, based on the complete reactions of sulfur with lithium metal to form Li_2S [1–3]. In addition, the cathode material sulfur also has the advantage of abundance in nature and low cost [4]. However, sulfur exhibits poor electrochemical activity for its insulating nature [5–8]. The lithium polysulfides generated during the charge/discharge process is soluble in the organic liquid electrolyte. The dissolved polysulfides are able to transfer to the lithium anode by a shuttle mechanism and cause lithium corrosion, which is ascribed to the capacity fading [9]. Numerous studies focused on diminishing the negative effect of the polysulfides shuttle by retaining the polysulfides at the cathode region through high surface-area adsorbents. Conductive polymer [10,11], active carbon [12], and multiwalled carbon tube [13] have been reported as an absorbing agent in lithium/sulfur battery due to their strong absorbing ability to the polysulfides and high electronic conductivity. However, the microstructure of the conducting agent needs to be optimized to satisfy the ions transportation during the repeated charge/discharge process. It should have enough space to carry the electrochemical active sulfur and maintain intimate contact with sulfur. Recent reports suggest that porous carbon is a promising matrix for sulfur [14–16]. This is because that the porous carbon could provide an extremely high surface area to disperse sulfur. However, the structure of the most reported porous carbon could not disperse sulfur homogenously for the lack of uniform holes. Therefore, it is a key to design an ordered structure for the porous carbon to ensure a well dispersion of sulfur.

In this study, ordered mesoporous carbon spheres (OMCs) with uniform penetrating channels were employed to act as the conductive agent. Active sulfur was highly dispersed in the channels and maintained intimate contact with the electrically conductive matrix. To further alleviate the polysulfides shuttle, all-solid-state $PEO_{18}Li(CF_3SO_2)_2N$–10 wt%SiO_2 electrolyte was used to replace the commercial organic electrolyte and it can be acted as a barrier to trap polysulfides at the cathode side. As a result, the lithium sulfur battery showed an improved cycling performance.

2. Experimental

The ordered mesoporous carbon spheres (OMCs) were synthesized with spherical mesoporous silica as a hard template [17]. S-OMCs composite was synthesized by heating the mixture of sulfur and OMCs at 155 °C for 4 h under N_2 protection. Sulfur has the lowest viscosity at 155 °C and can penetrate into the channels of the OMCs. The sulfur content in the S-OMCs composite measured by TG–DSC was about 67 wt%. The specific surface area of the as-prepared OMCs measured by BET testing was 1340.2 m^2 g^{-1}, and 440.2 m^2 g^{-1} for the S-OMCs composite. The sample was characterized by X-ray diffraction (XRD, Rigaku RINT-2000) with Cu

* Corresponding author. Tel.: +86 21 52411704; fax: +86 21 52413903.
E-mail addresses: zywen@mail.sic.ac.cn (Z. Wen), yuliu@mail.sic.ac.cn (Y. Liu).

0378-7753/$ – see front matter © 2010 Elsevier B.V. All rights reserved.
doi:10.1016/j.jpowsour.2010.12.052

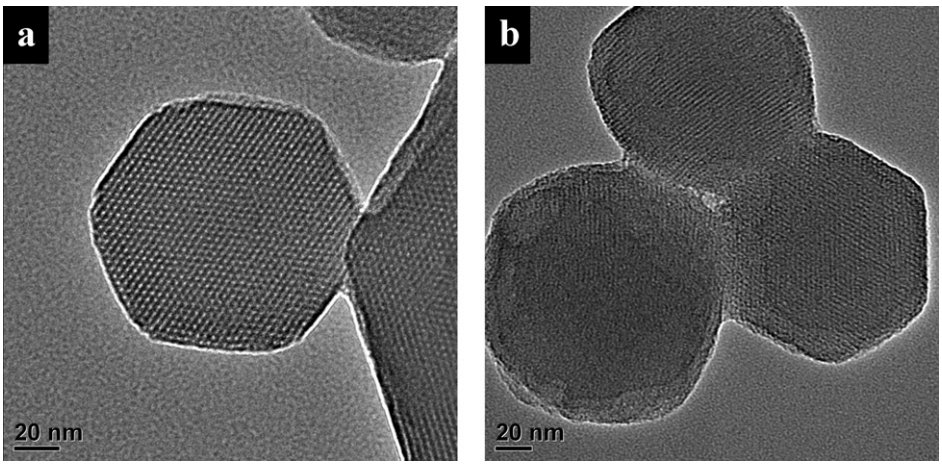

Fig. 1. TEM micrographs of the as-prepared OMCs (a) and S-OMCs (b).

Kα radiation to identify the phases formed. Transmission electron microscope (TEM JEM-2010) was applied to observe the morphology the as-prepared materials.

$PEO_{18}Li(CF_3SO_2)_2N$–10 wt%SiO_2 electrolyte was prepared in an argon-filled glove box. The stoichiometric PEO ($M_w = 6 \times 10^5$) and $Li(CF_3SO_2)_2N$ were dissolved in acetonitrile and SiO_2 powder was further added. The slurry was stirred for 12 h and cast on a Teflon sheet, and then was kept stationarily for 12 h. After the solvent evaporated at 65 °C, the electrolyte film was dried under vacuum at 90 °C for 12 h to remove the residual solvent. The conductivity of the PEO electrolyte is 5×10^{-4} S cm^{-1} at 70 °C.

Electrode containing 60 wt% of the as-prepared S-OMCs composite, 20 wt% PEO binder and 20 wt% acetylene black was made by coating the slurry of electrode components in acetonitrile onto aluminum foil and dried at 60 °C under vacuum for 12 h. Pristine sulfur cathode with the same sulfur content was also prepared for comparison. 2025 coin cells were assembled by sandwiching the PEO electrolyte film (0.18 mm) between a lithium foil and the as prepared sulfur cathode. The galvanostatic charge/discharge tests were conducted on a LAND CT2001A battery test system in a voltage range of 1.0–3.0 V (vs. Li/Li$^+$) at a current density of 0.1 mA cm^{-2}. AC impedances were measured by a Frequency Response Analyzer (FRA) technique on an Autolab Electrochemical Workstation over the frequency range from 0.01 to 10^6 Hz. The cyclic voltammetry experiments were performed on a CHI604 Electrochemical Workstation with a scan rate of 0.5 mV s^{-1}. All the cells were tested at 70 °C.

3. Results and discussion

Fig. 1a shows the TEM images of the as-prepared ordered mesoporous carbon sphere (OMC). The average diameter of the carbon sphere is approximately 120 nm. The mesoporous channels are arranged uniformly through the sphere. The center-to-center pore distance is about 5 nm. After the sublimed sulfur penetrated into the channels of the OMCs by heating, the ordered pattern of the outside and inner channels of the carbon spheres turned into ambiguity, as shown in Fig. 1b. Comparison of the TEM images of the OMCs with the S-OMCs composite accordingly confirmed that sulfur was loaded in the channels of the OMCs.

The XRD patterns of the as-prepared S-OMCs composite and OMCs are shown in Fig. 2. Both the sublimed sulfur and the sulfur in the S-OMCs composite belong to the Fddd orthorhombic crystal system, indicating that the sulfur loading process for the S-OMCs composite did not bring any structure change for sulfur.

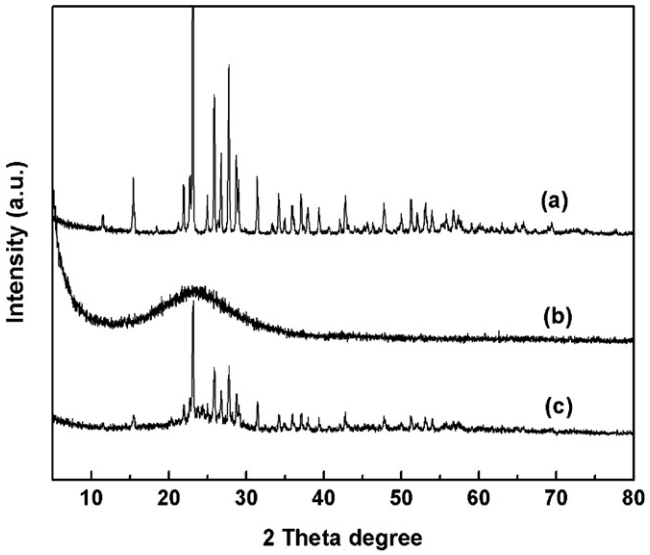

Fig. 2. XRD patterns of the sublimed sulfur (a), the as prepared OMCs (b) and the S-OMCs (c).

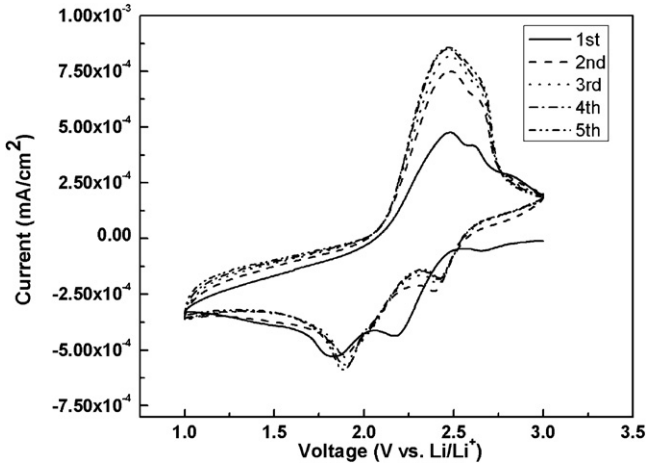

Fig. 3. CV curves of the S-OMCs composite cathode with PEO-based electrolyte at a scan rate of 0.5 mV s^{-1}, tested at 70 °C.

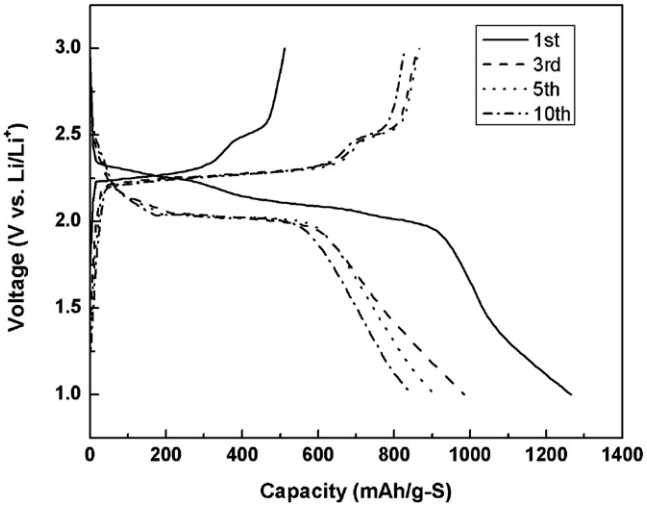

Fig. 4. Charge/discharge curves of the S-OMCs composite cathode vs. Li at current density of 0.1 mA cm^{-2}, tested at 70 °C.

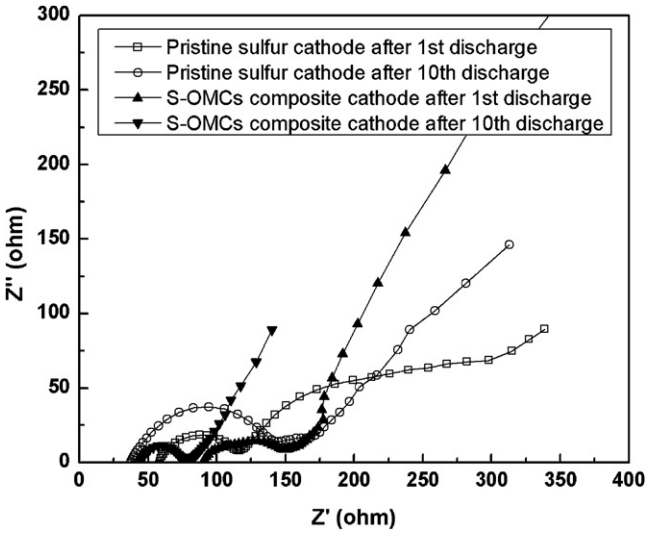

Fig. 5. EIS spectrum for the Li/S half cell with S-OMCs composite and pristine sulfur as cathode between 0.01 and 10^6 Hz, tested at 70 °C.

Cyclic voltammogram of the S-OMCs composite is given in Fig. 3. The material exhibits two pairs of reversible peaks, which are assigned to the typical responses of the two step reactions of sulfur with lithium [18]. As demonstrated above, the sulfur was highly trapped in the channels of the OMCs matrix. Therefore, the electrochemical reactions between sulfur and lithium during the first discharge process might overcome the strong absorbing energy of the OMCs, resulting in a shift towards a lower potential for the cathodic peak at 1.8 V vs. Li/Li$^+$ [7,12]. The current of the anodic peak for the S-OMCs increased slightly with initial several cycles and then remained to be constant, implying an activation process during the lithium ion insertion/extraction process. Compared with the lithium sulfur battery with organic liquid electrolyte, the cathodic peak at ca. 2.4 V for the S-OMCs composite based on all-solid-state PEO electrolyte still existed during all the cycles [7,16].

Fig. 4 shows the charge and discharge curves of the S-OMCs composite vs. Li/Li$^+$. The charge/discharge curves represented a typical characterization of Li/S batteries [7–16]. Two discharge voltage plateaus at ca. 2.3 V and ca. 2.0 V were observed. It was accordance with the CV measurements in Fig. 3. The initial discharge capacity is about 1265.5 mAh g^{-1} with an initial coulombic efficiency of ca. 70%. It is widely reported that lithium sulfur battery shows low efficiency at the first few cycles [7,10,12]. Poor interface between the electrolyte and Li anode is believed to plays an important role to the low efficiency. Moreover, the low efficiency is also attributed by the sulfur cathode. The volume change of the sulfur cathode during cycling could lead to the poor contact of the active sulfur and the PEO electrolyte [19].

Impedance spectrums of the Li/S half cell with the S-OMCs composite were compared to that based on the pristine sulfur, as shown in Fig. 5. The bulk resistances of both cells at high frequency decreased dramatically with the cycles. It was due to the gradually reduced thickness of the solid electrolyte arising from the flexibility of PEO at 70 °C under a high pressure on its sides in the testing cells. The semi-circles at higher frequency are corresponding to the charge transfer resistance (Rct) at the interface of cathode/PEO electrolyte and the inclined line in low frequency region is the diffusion impedance of lithium atoms in the composite (Warburg effect). The pristine sulfur showed an increased Rct after the first cycles. On the contrary Rct of the S-OMCs composite decreased dramatically with cycles and was much lower than that of the pristine sulfur. It suggests that the composite structure of S-OMCs is favorable for obtaining an improved interfacial compatibility with the all-solid-state PEO electrolyte compared to pristine sulfur.

The cycling performance of the S-OMCs composite was compared to that of the pristine sulfur, as shown in Fig. 6. The S-OMCs composite exhibits excellent cycling durability. The discharge capacity remained to be ca. 800 mAh g^{-1} after 25 cycles vs. 1265.5 mAh g^{-1} at the first cycle, meaning the capacity retention rate of ca. 65%. In contrast, pristine sulfur shows a poor cycling stability with a rapid discharge capacity fading. After 25 cycles the capacity retention was only 22%, meaning that the discharge capacity decreased from 1100 mAh g^{-1} at the first cycle to 240 mAh g^{-1} at the 25th cycle. The obvious improvement of the cycling stability of the S-OMCs composite would be attributed to several factors. The highly dispersed sulfur in the nanosized channels of the OMCs can successfully alleviate the volume effects of the Li/S electrochemical reaction. The large specific surface area originated from the uniform mesoporous channels in the OMCs can restrict the diffusion of the polysulfides during the charge/discharge process, which was proved by the EDS analysis of the sulfur content on the surface of the lithium anodes after 10 cycles with different cathodes. As shown in Fig. 7, the sulfur on the lithium with S-OMCs cathode is much lower than that of the lithium with pristine sulfur cathode.

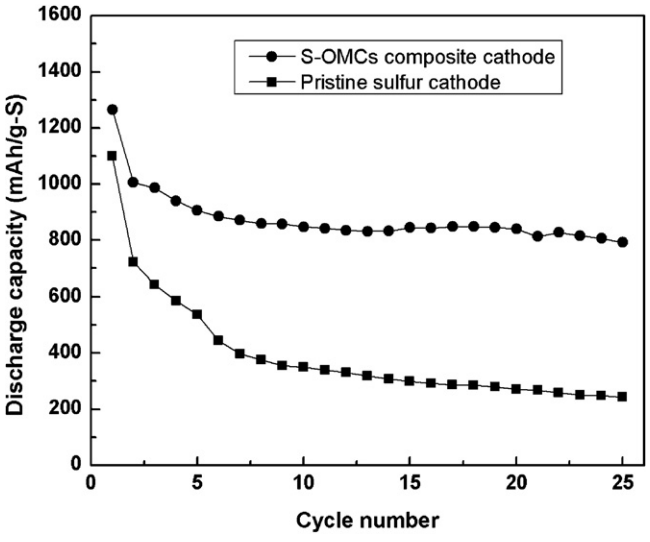

Fig. 6. Cycling performance of the Li/S half cell with S-OMCs composite and pristine sulfur as cathode, 0.1 mA cm^{-2}, tested at 70 °C.

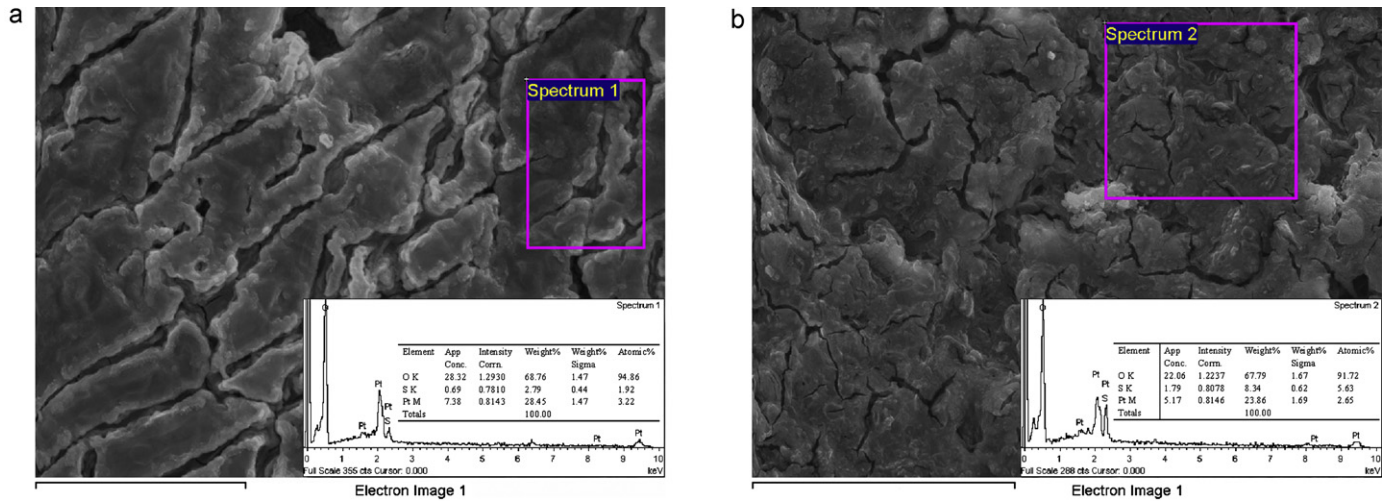

Fig. 7. EDS spectrums of the surface of the lithium anode with (a) S-OMCs composite cathode, and (b) with pristine sulfur cathode, the scale bar is 50 μm.

In addition, the intimate contact of the nano-dispersed sulfur with the OMCs matrix can highly ensure a good electrical path for the active sulfur during the repeated charge/discharge processes.

4. Conclusion

Mesoporous carbon sphere with the uniform channels (OMCs) was employed as the conductive agent in the sulfur cathode for the lithium sulfur battery based on all-solid-state $PEO_{18}Li(CF_3SO_2)_2N$–10 wt%SiO_2 electrolyte. Sulfur was penetrated into the channels of the OMCs by a co-heating method. Owing to the proper structure of the conductive matrix of OMCs as well as its intimate contacting with sulfur, the S-OMCs composite exhibits excellent cycling performance compared with the pristine sulfur. A reversible discharge capacity of about 800 mAh g^{-1} after 25 cycles was obtained. The S-OMCs composite is a promising cathode material for rechargeable lithium sulfur battery.

Acknowledgements

This work was financially supported by NSFC Project No. 50730001; research projects of Chinese Science and Technology Ministry No. 2007BAA07B01 and No. 2007CB209700; research projects from the Science and Technology Commission of Shanghai Municipality No. 08DZ2210900 and No. 09PJ1410800.

References

[1] J.L. Wang, J. Yang, J.Y. Xie, N.X. Xu, Adv. Mater. 14 (2002) 963.
[2] L.X. Yuan, J.K. Feng, X.P. Ai, Y.L. Cao, S.L. Chen, H.X. Yang, Electrochem. Commun. 8 (2006) 610.
[3] Y. Jung, S. Kim, Electrochem. Commun. 9 (2007) 249.
[4] H. Yamin, E. Peled, J. Power Sources 9 (1983) 281.
[5] Y.-J. Choi, Y.-D. Chung, C.-Y. Baek, K.-W. Kim, H.-J. Ahn, J.-H. Ahn, J. Power Sources 184 (2008) 548.
[6] X.L. Ji, K.T. Lee, F. Linda, L.F. Nazar, Nat. Mater. 8 (2009) 500.
[7] B. Zhang, C. Lai, Z. Zhou, X.P. Gao, Electrochim. Acta 54 (2009) 3708.
[8] K. Kumaresan, Y. Mikhaylik, R. White, J. Electrochem. Soc. 155 (2008) A576.
[9] Y.V. Mikhaylik, J.R. Akridge, J. Electrochem. Soc. 151 (2004) A1969.
[10] J. Wang, J. Chen, K. Konstantinov, L. Zhao, S.H. Ng, G.X. Wang, Z.P. Guo, H.K. Liu, Electrochim. Acta 51 (2006) 4634.
[11] M.M. Sun, S.C. Zhang, T. Jiang, L. Zhang, J.H. Yu, Electrochem. Commun. 10 (2008) 1819.
[12] J.L. Wang, J. Yang, J.Y. Xie, N.X. Xu, Y. Li, Electrochem. Commun. 4 (2002) 499.
[13] L.X. Yuan, H.P. Yuan, X.P. Qiu, L.Q. Chen, W.T. Zhu, J. Power Sources 189 (2009) 1141.
[14] C.D. Liang, N.J. Dudney, J.Y. Howe, Chem. Mater. 21 (2009) 4724.
[15] J. Wang, S.Y. Chew, Z.W. Zhao, S. Ashraf, D. Wexler, J. Chen, S.H. Ng, S.L. Chou, H.K. Liu, Carbon 46 (2008) 229–235.
[16] C. Lai, X.P. Gao, B. Zhang, T.Y. Yan, Z. Zhou, J. Phys. Chem. C 113 (2009) 4712.
[17] J.H. Zhou, J.P. He, C.X. Zhang, T. Wang, D. Sun, Z.Y. Di, D.Y. Wang, Mater. Charact. 61 (2010) 31.
[18] D. Marmorstein, T.H. Yu, K.A. Striebel, E.J. Cairns, J. Power Sources 89 (2000) 219.
[19] X.M. He, J.G. Ren, L. Wang, W.H. Pu, C.Y. Jiang, C.R. Wan, J. Power Sources 190 (2009) 154.